An approach to study ultrastructural changes and adaptive strategies displayed by Acinetobacter guillouiae *SFC 500-1A under simultaneous Cr(VI) and phenol treatment*

Marilina Fernández, Gustavo M. Morales, Elizabeth Agostini & Paola S. González

Environmental Science and Pollution Research

ISSN 0944-1344

Environ Sci Pollut Res
DOI 10.1007/s11356-017-9682-1

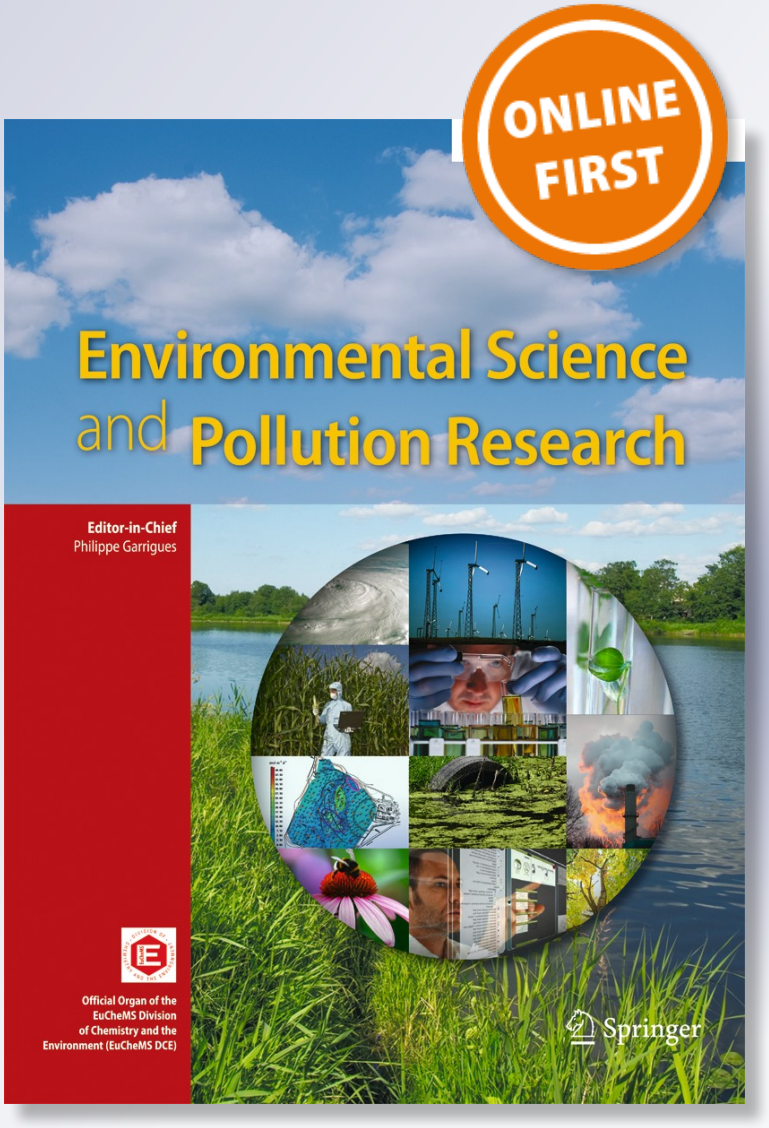

Springer

Environ Sci Pollut Res
DOI 10.1007/s11356-017-9682-1

RESEARCH ARTICLE

An approach to study ultrastructural changes and adaptive strategies displayed by *Acinetobacter guillouiae* SFC 500-1A under simultaneous Cr(VI) and phenol treatment

Marilina Fernández[1] · **Gustavo M. Morales**[2] · **Elizabeth Agostini**[1] · **Paola S. González**[1]

Received: 2 March 2017 / Accepted: 29 June 2017

Abstract *Acinetobacter guillouiae* SFC 500-1A, a native bacterial strain isolated from tannery sediments, is able to simultaneously remove high concentrations of Cr(VI) and phenol. In this complementary study, high-resolution microscopy techniques, such as atomic force microscopy (AFM) and transmission electron microscopy (TEM), were used to improve our understanding of some bacterial adaptive mechanisms that enhance their ability to survive. AFM contributed in gaining insight into changes in bacterial size and morphology. It allowed the unambiguous identification of pollutant-induced cellular disturbances and the visualization of bacterial cells with depth sensitivity. TEM analysis revealed that Cr(VI) produced changes mainly at the intracellular level, whereas phenol produced alterations at the membrane level. This strain tended to form more extensive biofilms after phenol treatment, which was consistent with microscopy images and the production of exopolysaccharides (EPSs). In addition, other exopolymeric substances (DNA, proteins) significantly increased under Cr(VI) and phenol treatment. These exopolymers are important for biofilm formation playing a key role in bacterial aggregate stability, being especially useful for bioremediation of environmental pollutants. This study yields the first direct evidences of a range of different changes in *A. guillouiae* SFC 500-1A which seems to be adaptive strategies to survive in stressful conditions.

Keywords Chromium · Phenol · AFM · Exopolymers · Biofilm

Responsible editor: Diane Purchase

Electronic supplementary material The online version of this article (doi:10.1007/s11356-017-9682-1) contains supplementary material, which is available to authorized users.

✉ Paola S. González
pgonzalez@exa.unrc.edu.ar

Marilina Fernández
mfernandez@exa.unrc.edu.ar

Gustavo M. Morales
gmoralesexa@gmail.com

Elizabeth Agostini
eagostini@exa.unrc.edu.ar

[1] Departamento de Biología Molecular, FCEFQyN, Universidad Nacional de Río Cuarto (UNRC), Ruta 36 Km 601, 5800 Río Cuarto, Córdoba, Argentina

[2] Departamento de Química-FCEFQyN, Universidad Nacional de Río Cuarto, 5800 Río Cuarto, Córdoba, Argentina

Introduction

Hexavalent chromium Cr(VI) and phenol are discharged from several industrial effluents, and they are listed as priority pollutants by the US Environmental Protection Agency due to their high toxicity and persistence (ATSDR 2005; Dhal et al. 2013). Several methods have been proposed for their elimination; however, bioremediation could be considered as a novel, efficient, eco-friendly, and cost-effective strategy for the treatment of such environmental pollutants by using microorganisms (Dhal et al. 2013). In this context, we isolated a bacterial strain from tannery sediments, identified as *Acinetobacter guillouiae* SFC 500-1A, which was able to simultaneously remove high Cr(VI) and phenol concentrations. The mechanisms involved in Cr(VI) removal and phenol biodegradation were recently studied (Ontañon et al. 2015). However, more

Published online: 13 July 2017

studies are needed in order to improve our understanding of morphological and ultrastructural changes, properties of microbial cell surfaces, and the mechanisms involved in the adaptation to such polluted environments. In addition, until now, studies that reveal changes in cell morphology of bacteria exposed to different environmental stresses only focus on bacterial length regardless of other parameters, such as width and height of the cell. Therefore, it is necessary to deepen some lesser known aspects.

Actually, techniques based on atomic force microscopy (AFM) have revolutionized the characterization of microbial cells. They have already delivered important information on real-time interaction, both under physiological conditions and also under external stimuli (Dufrêne 2014). In particular, AFM has been mostly used to analyze bacterial responses to lytic bacteriophages or antibiotics (Dubrovin et al. 2012; Longo and Kasas 2014). Nevertheless, it has been less used to study bacterial responses to environmental contaminants, hence the novelty of the present research.

In co-polluted environments, microorganisms develop survival strategies against these adverse conditions, such as biofilm formation (Busscher and Mei 2012). Biofilms can be described as a microbially derived sessile community characterized by cells attached to a surface, which are embedded in a matrix of extracellular polymeric substances. This matrix is usually composed of exopolysaccharides (EPSs), proteins, and sometimes nucleic acids (Strelkova et al. 2013). EPS could protect bacterial cells from desiccation, heavy metals, organic compounds, or other environmental stressors (Hung et al. 2005). In addition, it has been found that EPS has metal-binding properties or the capability to sequestrate metals or other compounds (Harish et al. 2012). Thus, the binding of these compounds by EPS is thought to be an important mechanism for pollutant detoxification of contaminated sites (Hu et al. 2007). However, it should not minimize the possible role of proteins and DNA, present in the extracellular matrix, in the remediation process. Besides that, certain physiological properties of bacterial cells such as hydrophobicity were found to influence the bacteria-pollutant interaction, suggesting that hydrophobic forces could also play an important role in the bioremediation of contaminants.

Therefore, the aim of this work was to investigate some resistance mechanisms developed by *A. guillouiae* SFC 500-1A after simultaneous exposure to Cr(VI) and phenol, which involve morphological and ultrastructural changes using scanning electron microscopy (SEM), transmission electron microscopy (TEM), and AFM in order to provide new insights on the structure and function of microbial cell surfaces. The ability of biofilm formation, as well as exopolymer production (EPS, proteins, DNA) and cell hydrophobicity, was also analyzed. This study could contribute to develop a more effective technology and to overcome some of the present limitations of bacterial bioremediation.

Materials and methods

Biological, material, and culture conditions

A. guillouiae SFC 500-1A isolated from contaminated tannery sediments was used in this study (Ontañon et al. 2015). The strain was maintained in TY medium (Beringer 1974) at 28 ± 2 °C and subcultured weekly.

For the different experiments, the strain was grown in TY medium supplemented with Cr(VI) (25 mg L^{-1}) or phenol (300 mg L^{-1}) and both contaminants simultaneously. These concentrations were selected based on previous studies (Ontañon et al. 2015). Erlenmeyer flasks containing 20 mL of TY medium were inoculated (10% *v*/*v*) with a bacterial culture grown overnight, until late exponential phase. Then, they were incubated at 28 ± 2 °C and 200 rpm, during 16 h. Cr(VI) was determined according to APHA (APHA-AWWA 1998), while phenol was evaluated by a spectrophotometric method (Wagner and Nicell 2002).

In each experiment, Erlenmeyer flasks with TY medium supplemented with Cr(VI) or phenol and both contaminants simultaneously were carried out and used as abiotic controls, to evaluate possible losses of the contaminants by physicochemical processes.

Study of structural and ultrastructural changes in *A. guillouiae* SFC 500-1A

Atomic force microscopy

In order to evaluate the effect of Cr(VI), phenol, and a mixture of both contaminants on the morphology and surface characteristics, cells were exposed to these pollutants during 16 h. Then, the culture was diluted to obtain an optical density (OD_{600}) of 0.4. A volume of 200 μL was harvested, washed three times with Milli-Q water, and resuspended in 200 μL. An aliquot (20 μL) of this suspension was immobilized on a glass coated with polyethyleneimine (PEI) for AFM study. The glass substrate was washed with potassium hydroxide/ethanol solution (1:3), followed by exhaustive washing with Milli-Q water, immersed in a PEI dispersion (0.1% (*v*/*v*), PEI branched, MW ~25,000, Sigma-Aldrich) for 1 min, subsequently rinsed with deionized water for 5 min, and dried under a stream of nitrogen (Morris et al. 1999; Dufrene 2008). The cells were immobilized by spreading them on the support, allowed to stand for 20 min at 28 °C, rinsed with deionized water, and mounted for observation. The images were obtained by AFM (Agilent Technologies SPM, model 5500), working in acoustic mode, using a probe (Micromasch, HQ:XSC11/A1 BS) with a cantilever resonance frequency and force constant of 155 kHz and 7 N m^{-1}, respectively. The width, length, and height diameter of 63 microorganisms were measured by using Gwyddion v. 2.39, a software for

scanning probe microscopy data visualization and analysis. Results of length, width, and height ranges were extracted from frequency graphs (Online Resource).

Transmission electron microscopy

Ultrastructural changes of cells grown in the presence of Cr(VI), phenol, and both contaminants during 16 h were studied using TEM (JEOL JEM 12EXII, Japan). The bacterial culture was centrifuged, and the pellet was fixed using 2.5% glutaraldehyde in *s*-collidine buffer solution (0.2 M, pH 7.4) for 3 h at 4 °C. Then, the cells were washed with the *s*-collidine buffer solution and fixed with 1% osmium tetraoxide. Fixed samples were dehydrated with acetone. The pre-inclusion was made with 812 1:1 EMbed epoxy resin in 100% acetone and the inclusion with EMbed 812 at 56 °C. Semi-thin sections were cut using a manual ultramicrotome (Sorvall MT-1A, DuPont), and they were stained with toluidine blue and observed under optical microscope. Ultrathin sections (20–60 nm) were performed with diamond blade (PelcoR), and they were placed on copper grids and contrasted with uranyl acetate and lead citrate (Bencosme and TsutSumi 1970; Ackerley et al. 2006).

Scanning electron microscopy

The cells of *A. guillouiae* SFC 500-1A were exposed to the contaminants as was previously described. The bacterial culture was centrifuged, and the pellet was fixed with 2.5% glutaraldehyde for 12 h at 4 °C, followed by rinsing with distilled water. Later, it was dehydrated using solutions with increasing ethanol concentrations, dried and fixed with double-sided tape on aluminum, and coated with gold, Denton Vacuum Desk IV (22–24 nm thick). Finally, the samples were examined using SEM.

Exopolymer production: quantification of exopolysaccharides, proteins, and DNA

The bacterial cultures exposed to different contaminants for 16 h were centrifuged at 10,000 rpm, for 15 min at 4 °C, and the pellets were dried at 60 °C, until constant weight. The exopolymers were extracted by the modified procedure of Mueller and González (2011). EPS quantification was carried out by the anthrone method, and a calibration curve was performed using glucose (1 mg mL^{-1}) (Dische 1962). The results were expressed as grams of EPS per gram of dry weight. Proteins were estimated according to Bradford (1976), using bovine serum albumin (0.1 mg mL^{-1}) as standard, and the results were expressed as micrograms of protein per microliter. DNA was quantified by measuring the absorbance ratio at 260/280 nm, and the results were expressed as microgram of DNA per microliter.

Biofilm formation

Biofilm formation was determined by measuring the amount of cells attached to Khan's tube after 72 h, using the crystal violet 0.01% staining method (O'Toole and Kolter 1998). The stained biofilm ring was homogenized with 96% ethanol, and the $OD_{570\ nm}$ was measured using an ELISA reader (Multiskan™ FC Microplate Photometer, Thermo Scientific, USA). Besides, SEM was used to examine biofilm formation in all conditions.

Hydrophobicity determination

The ability of bacterial cells to adhere to hydrocarbon (xylene) was used as a measure of their hydrophobicity (Li and Mclandsborough 1999). The bacteria were exposed to the pollutants at different times to analyze changes in this property. An overnight culture of 10 mL was centrifuged at 10,000 rpm, for 15 min. Then, the pellet was washed three times with phosphate-buffered solution (PBS) and resuspended in the same buffer to obtain an $OD_{600\ nm}$ of 1.0. Samples of each suspension (3 mL) were added to 1 mL xylene and mixed during 5 min. The OD of the aqueous phase was measured at 600 nm after 20 min at room temperature. The percentage of hydrophobicity (% h) was determined using the following equation:

$$\%h = [(A_i - A_f) \times 100]/A_i.$$

where A_i corresponds to the initial bacterial cell absorbance and A_f corresponds to the absorbance of aqueous phase after mixing with xylene.

Statistical analysis

All experiments were performed three times in independent assays. The results were presented as the mean and standard error. Statistical analysis was carried out using analysis of variance. To determine significant differences between treatments, Tukey test was applied, with a significance level of 0.05 ($p < 0.05$) by using software R (version 3.1.1).

Results and discussion

Effect of Cr(VI) and phenol on cell morphology and structure of *A. guillouiae* SFC 500-1A

The effect of Cr(VI), phenol, and both contaminants on cell morphology and surface topology of *A. guillouiae* SFC 500-1A was examined by AFM. The bacterial cells, growing in control conditions, showed morphological characteristics of Gram-negative cocci or coccobacilli (Fig. 1a, b). Frequency

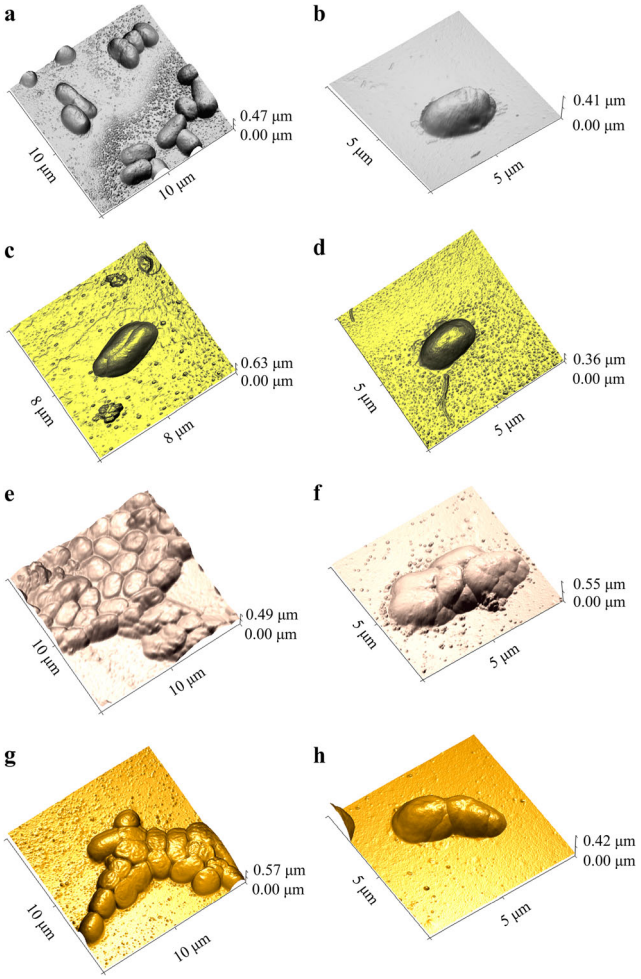

Fig. 1 Morphology of *A. guillouiae* SFC 500-1A by AFM growing in control condition (**a**, **b**) and in the presence of Cr(VI) (**c**, **d**), phenol (**e**, **f**), and both contaminants (**g**, **h**)

graphs showed that most of the analyzed cells reached a length range between 0.60 and 2.40 μm, width between 0.60 and 1.35 μm, and height between 0.20 and 0.36 μm (Table 1). When the bacteria were treated with Cr(VI) (25 mg L^{-1}), the cells increased their size, showing an increase in length, width, and height. Most cells showed lengths between 0.90 and 1.80 μm; however, cells with a length up to 3.60 μm were also observed (Online Resource). These cell elongation and size increase observed in *A. guillouiae* SFC 500-1A were also reported for other *Acinetobacter* species, as well as for other bacterial strains exposed to chromium (Li et al. 2008; Samuel et al. 2012). The analysis of the cell surface, at different growth conditions, showed no significant changes, regardless of whether or not Cr was present in the culture (Fig. 2a–d). By contrast, *Acinetobacter haemolyticus* and *Bacillus cereus* SJ1 showed a remarkable appearance of wrinkles and enhanced roughness on the cell surface when they were cultivated with K_2CrO_4 (Zakaria et al. 2007; He et al. 2010). When *A. guillouiae* SFC 500-1A was exposed to phenol, cells tended to form aggregates and increased their size compared to cells grown under control conditions (Fig. 1e, f; Table 1). The largest number of cells showed a length range of 0.90–2.70 μm and a cell width from 0.90 to 1.05 μm. Similarly, a significant increase was observed in cell height, which varied from 0.32 to 0.48 μm (Online Resource). Phenol also induced substantial modifications on cell surface morphology (Fig. 2e, f). The formation of large cell aggregates was also reported for *Pseudomonas putida* CP1 during growth with phenols and monochlorophenols (Farrell and Quilty 2002; Sidek 2010). Thereby, the observed cell aggregation could be a microbial strategy to increase tolerance against pollutant toxicity.

Finally, it was observed that the bacteria changed their size and morphology, and also, they formed cellular aggregates, after simultaneous exposure to Cr(VI) and phenol (Fig. 1g, h). Moreover, important differences in length, width, and height were observed. Most of the cells showed lengths in a frequency range between 1.20 and 1.80 μm and width and height ranges between 1.05 and 1.20 and 0.28 and 0.40 μm, respectively (Online Resource). Cell surface roughness was similar to those observed after phenol treatment (Fig. 2g, h). These morphological changes could reflect the presence of extracellular polysaccharides, according to Francius et al. (2008). To the best of our knowledge, this is the first time that morphological changes of bacterial cells produced by Cr(VI) and phenol are studied using AFM, providing interesting evidences of their effects on bacterial size which could be related to adaptation mechanisms against pollutants.

Transmission electron microscopy analysis

Transmission electron images of bacterial cells after pollutant treatment give the possibility to study cell physiology and especially changes in cell ultrastructure, as shown in Fig. 3. When the bacteria were grown in control conditions, the cell membrane was well defined and a smooth and clear cytoplasm (CC) was observed, with few electron-dense particles (EDPs) (Fig. 3a). These precipitates could correspond to Cr, due to the fact that cells were maintained by weekly subculture in TY medium with chromium and phenol. However, cells were grown in TY medium without contaminants in those experiments under control conditions. Deposition of such precipitates was also observed in *Pseudomonas aeruginosa* Rb-1 and *Ochrobactrum intermedium* Rb-2, even when cells grew in Cr(VI) absence (Batool et al. 2014).

Upon exposure to Cr(VI), *A. guillouiae* SFC 500-1A showed considerable morphological modifications, such as the increment in size and a reduced dark cytoplasmic (DC) space or increased periplasmic space by the detachment of the inner membrane (IMD). Besides, a large number of electron-dense precipitates were observed. Possibly, the electron-opaque particles could be attributable to chromium precipitation. For instance, intracellular localization of electron-dense precipitates indicated the intracellular reduction of Cr(VI) to

Table 1 Length, width, and height ranges of *A. guillouiae* SFC 500-1A exposed to different contaminants (Cr(VI) 25 mg $L^{-1}$and phenol 300 mg L^{-1})

Culture condition	Length ranges (μm)	Width ranges (μm)	Height ranges (μm)
Control	0.60–2.40	0.60–1.35	0.20–0.36
Cr(VI)	0.60–3.60	0.60–1.65	0.20–0.40
Phenol	0.60–2.70	0.60–1.65	0.24–0.52
Cr(VI) + phenol	0.90–3.60	0.75–1.65	0.24–0.48

Ranges were extracted from frequency graphs (Online Resource)

Cr(III) in *Shewanella oneidensis*, *Acinetobacter* sp. PCP3, and *P. putida*. Subsequently, Cr(III) could interact with specific binding sites (Daulton et al. 2001; Srivastava and Thakur 2007). As was previously demonstrated in our laboratory, *A. guillouiae* SFC 500-1A was able to intracellularly reduce Cr(VI) to Cr(III), which was mediated by chromate reductase activity (Ontañon et al. 2015). These observed inclusions were unevenly distributed in the cytoplasm, as well as associated with the periplasm and outer membrane, and even localized extracellularly (Fig. 3b). The adsorbed chromium to the membrane would be Cr(III), due to the inability of chromate anions to bind with the electronegative functional groups frequently found on Gram-negative envelopes (McLean and Beveridge 2001). Similar changes in morphology, cell surface, and distribution of electronic-dense precipitates have been observed in other *Acinetobacter* species as well as in *O. intermedium* Rb-2 grown in the presence of Cr(VI) (Francisco et al. 2010; Bhattacharya and Gupta 2013; Batool et al. 2014).

When the cells were exposed to phenol and both pollutants simultaneously, they showed a similar cytoplasmic appearance with control cells (Fig. 3c, d). However, the morphology of *A. guillouiae* SFC 500-1A changed after Cr(VI) and phenol treatment, which was coincident with the changes observed by AFM. From this result, we concluded that phenol addition affected size and cell surface but probably not the cell ultrastructure (Figs. 1 and 2e, f). In this context, Bhattacharya et al. (2014) reported that *Acinetobacter* sp. B9 showed Cr deposition and membrane disturbance, when it was simultaneously exposed to Cr(VI) and phenol. In addition, polyhydroxybutyrate (PHB) formation and irregular bulges at the plasma membrane were observed in *A. haemolyticus* cells, growing with phenol 100 and 1000 mg L^{-1}. The formation of blebs on the plasma membrane is one of the morphological changes shown by the cell when it undergoes apoptosis. This could be related to its inability to resist or detoxify phenol, which leads to cell death. Moreover, PHB production during growth with phenol is probably a detoxifying mechanism, because it could allow the bacteria to reduce the toxicity and cope with the stressed environment (Sidek 2010). These responses were not observed in *A. guillouiae* SFC 500-1A, probably because the phenol concentrations used in this work were not toxic for this strain, since phenol could be completely metabolized through the *ortho*-cleavage pathway (Ontañon et al. 2015). It is important to note that the exposure to both contaminants did not produce cell lysis of this strain as was also reported for *P. aeruginosa* Rb-1 and *O. intermedium* Rb-2 exposed to Cr(VI) (Batool et al. 2014).

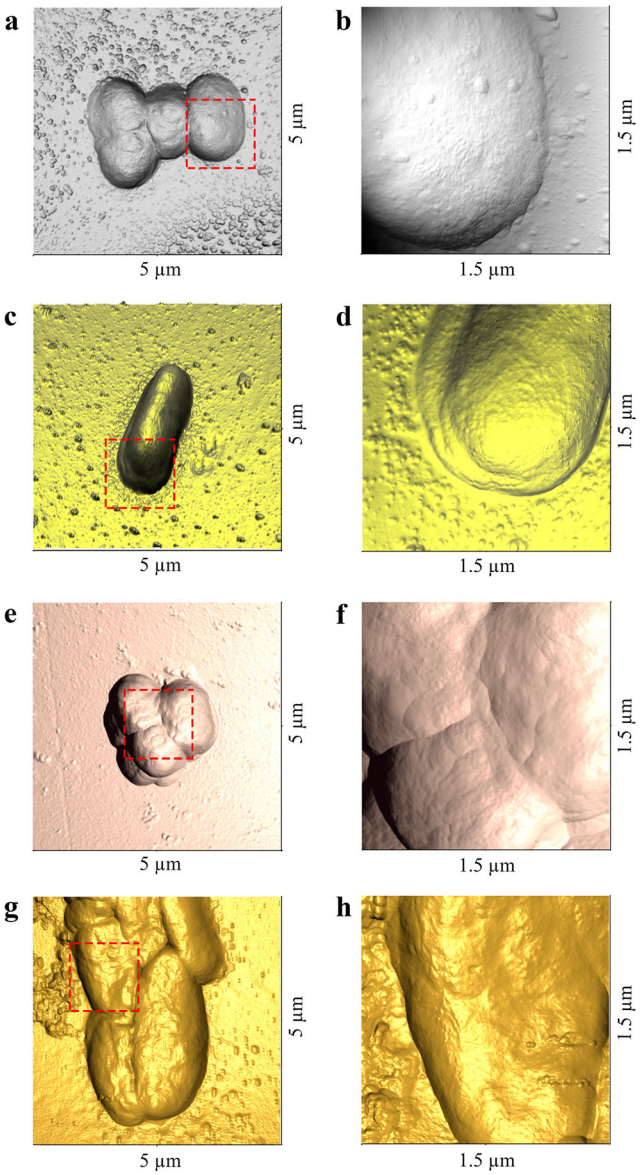

Fig. 2 Analysis of *A. guillouiae* SFC 500-1A cell surface by AFM, growing in control conditions (**a**, **b**) and in culture media supplemented with Cr(VI) (**c**, **d**), phenol (**e**, **f**), and both contaminants (**g**, **h**)

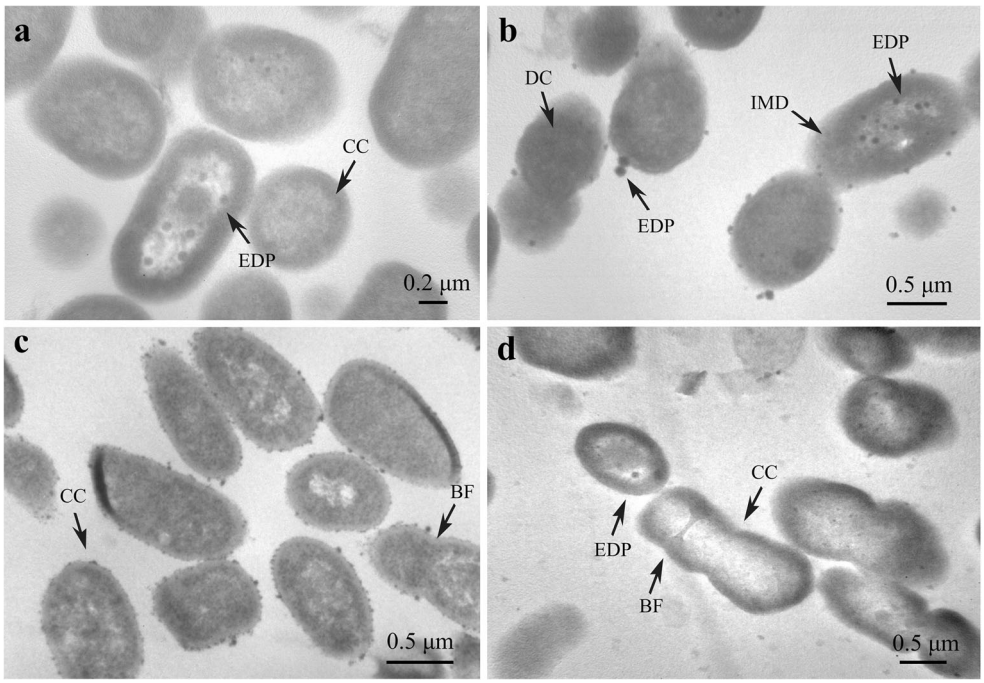

Fig. 3 Transmission electron microscopy of *A. guillouiae* SFC 500-1A cells growing in different conditions. **a** Control, **b** Cr(VI) 25 mg L^{-1}, **c** phenol 300 mg L^{-1}, and **d** Cr(VI) 25 mg L^{-1} and phenol 300 mg L^{-1} after 16 h. *EDP* electronic dense particle, *BF* binary fission, *CC* clear cytoplasm, *DC* dark cytoplasm, *IMD* possible detachment of inner membrane which leads to reduced cytoplasmic space or increased periplasmic space

In conclusion, both contaminants affected bacterial size; however, Cr(VI) mainly induced intracellular changes, whereas phenol produced changes at the membrane level.

Exopolymer isolation: quantification of exopolysaccharides, proteins, and DNA

The production of different exopolymer components of *A. guillouiae* SFC 500-1A exposed to the studied contaminants was evaluated. The bacteria removed 100% of phenol and 15 and 50% of Cr(VI), after treatments with Cr(VI) and with both pollutants, respectively. EPS production significantly increased in treatments with both compounds showing a synergistic effect (Fig. 4c, d). In the presence of Cr(VI), white incrustations were observed, which could be attributable to the binding of chromium ions on EPS surface (Sharma et al. 2008; Quintelas et al. 2011). On the other hand, the adhesive interaction between cells forming a characteristic biofilm was observed, after phenol treatment and with both pollutants simultaneously (Fig. 4e, f).

Extracellular polymeric substances are composed of different macromolecules, including not only polysaccharides but also proteins and nucleic acids, hence the importance of its determination. Table 2 shows protein, DNA, and Cr(VI) contents of the exopolymeric matrix. Protein concentration increased in all treatments compared to the control, the increase being more significant in the presence of both pollutants, while DNA content significantly increased in the presence of phenol and both pollutants, compared to the control. Furthermore, the concentrations of Cr(VI) in the exopolymer were around 0.5 and 1 mg L^{-1} after treatments with Cr(VI) and with Cr(VI) and phenol, respectively.

Dogan et al. (2015) showed a positive correlation between Cr(VI) tolerance and EPS production in *Bacillus licheniformis* B22. However, under the assayed conditions, *A. guillouiae* SFC 500-1A enhanced EPS production only when it grew in the presence of both contaminants. It is important to note that EPSs are capable of adsorbing different heavy metals, as was described for *Bacillus firmus* which was able to bind metal ions like Pb, Cu, and Zn (Salehizadeh and Shojaosadati 2003). For this reason, exopolymers play a crucial role in the biosorption/bioremediation of heavy metals especially chromium (Quintelas et al. 2011; Harish et al. 2012). EPS forms complexes with metal cations retarding their diffusion within the biofilm and produce their immobilization within the exopolymeric matrix (Pal and Paul 2008). These complexes generally result from electrostatic interactions, van der Waals' forces, and surface complexation between cationic metal ligands and negatively charged components of biopolymers (proteins and carbohydrates) like carboxyl (amino acids, uronic acids), phosphoryl, and sulfate groups (Santamaría et al. 2003; Guibaud et al. 2006).

Although a low Cr(VI) concentration was detected in the exopolymeric matrix of *A. guillouiae* SFC 500-1A, EPS could act as Cr(III) chelating, since chromium, added as a dichromate, could be reduced from anionic Cr(VI) to cationic Cr(III), which would interact with this negatively charged polymer. This hypothesis could be supported by recent studies that detected cytosolic chromate reductase activity in *A. guillouiae* SFC 500-1A (Ontañon et al. 2015). Contrarily, Prieto-Contreras et al. (2015) reported an increase of EPS in

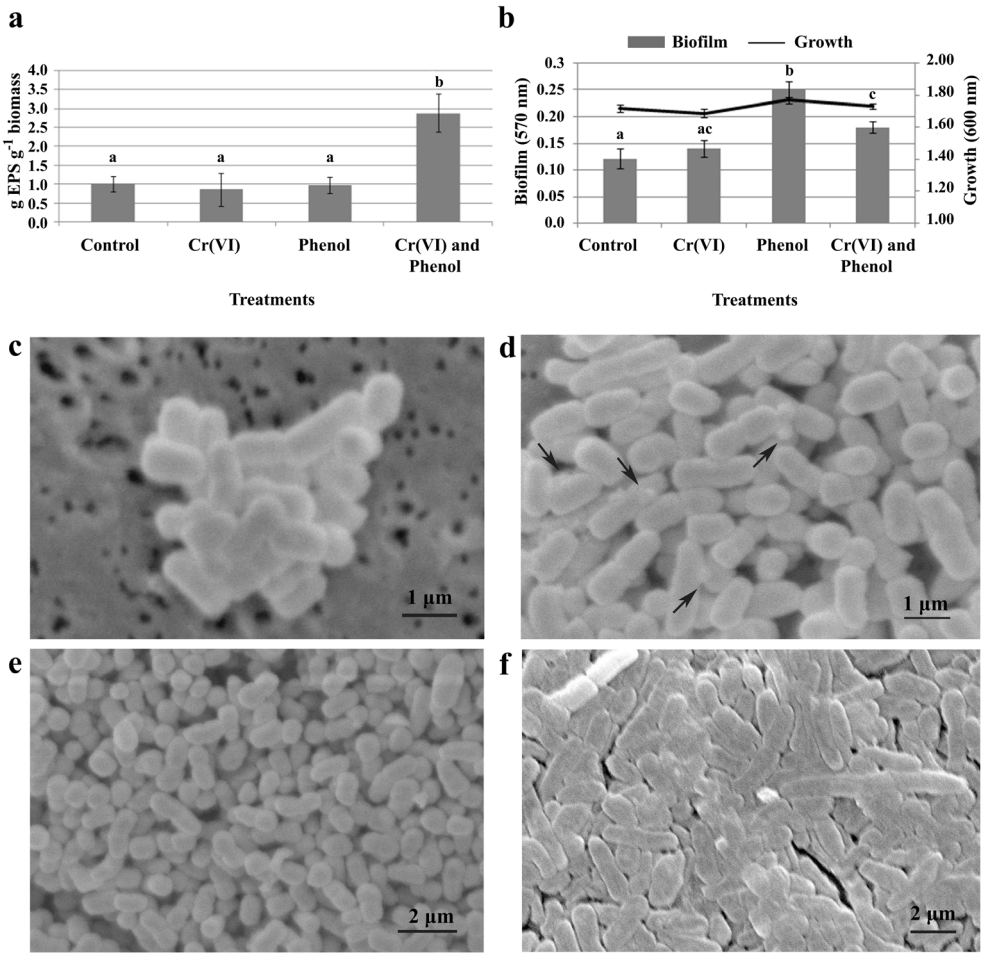

Fig. 4 EPS production and biofilm formation of *A. guillouiae* SFC 500-1A. **a** EPS production in the presence of Cr(VI) 25 mg L^{-1}, phenol 300 mg L^{-1}, and both pollutants Cr(VI) 25 mg L^{-1} and phenol 300 mg L^{-1}. **b** Biofilm formation of *A. guillouiae* SFC 500-1A exposed to the same conditions. **c** SEM analysis of cell growth in control condition, **d** with Cr(VI) (*arrows* would indicate metal binding to exopolymers), **e** with phenol, and **f** with Cr(VI)-phenol, in the same concentrations listed above

Acinetobacter sp. when higher Cr levels (153 mg L^{-1}) than those used in our experiments were added to the medium. Thus, the production of high levels of EPS could be related with the Cr concentration originally added.

Little is known about the mechanisms by which organic compounds interact with exopolymers. It is described that EPS production increased due to an increment in glucose concentration (Quintelas et al. 2011), resulting in an excess of carbon or limitations in nitrogen source, potassium, or phosphorus (Pal and Paul 2008). In our study, the addition of phenol to the culture medium involves an extra carbon supply, possibly creating an imbalance in the carbon-nitrogen relationship, which would increase EPS production in phenol-treated bacterial cells. Similarly, the overproduction of EPS was observed in *Acinetobacter* sp. strain DR1 after treatment with diesel oil and *n*-hexadecane (Kang and Park 2010), and several *Pseudomonas* species were able to produce EPS in the presence of various organic pollutants (2,4-D, benzene, BTX, and gasoline) (Onbasli and Aslim 2009). Moreover, in marine bacterial biofilms, an increase in EPS production was observed using seawater media containing toxic metals and chemicals, such as glutaraldehyde and phenol (Fang et al. 2002).

On the other hand, the exopolymer obtained after Cr(VI) and phenol treatment showed higher protein content than that obtained after Cr(VI) treatment. This could explain the greater quantification of Cr(VI) in the latter exopolymer, because the proteins of the extracellular polymeric matrix would be the major metal-binding component as was described for *Rhodopseudomonas acidophila* growing with Cu(II), Cd(II), and Cr(VI) (Sheng et al. 2005).

Nucleic acids present in the exopolymeric matrix of biofilms have been termed extracellular DNA (eDNA)

Table 2 Protein, eDNA, and Cr(VI) in the exopolymer of *A. guillouiae* SFC 500-1A

Condition component	Control	Cr(VI)	Phenol	Cr(VI) + phenol
Protein (µg $µL^{-1}$)	0.010 ± 0.002a	0.312 ± 0.280b	0.123 ± 0.094b	11.542 ± 0.440c
eDNA (µg mL^{-1})	5.2 ± 3.22a	21.5 ± 10.35a	39.2 ± 11.38ab	72.5 ± 18.49b
Cr(VI) (µg mL^{-1})	–	0.49 ± 0.03	–	0.82 ± 0.17

(Steinberger and Holden 2005). They have several functions within biofilm formation and maintenance including initial attachment and structural stability (Molin and Tolker-Nielsen 2003). In *A. guillouiae* SFC 500-1A, different DNA concentrations were detected in the exopolymeric matrix according to the applied treatment (Table 2). The presence of eDNA molecules on bacterial cell surfaces has been shown to increase bacterial cell surface hydrophobicity and therewith influences adhesion to substrate surfaces (Das et al. 2010) as well as between bacteria (aggregation) (Liu et al. 2008; Das et al. 2011). This could explain the aggregation between the cells of *A. guillouiae* SFC 500-1A in treatments with phenol and both pollutants (Figs. 1e–h, 2e–h, and 4e, f), coinciding with those treatments where higher contents of eDNA were quantified. It has been reported that, at high eDNA concentrations, metal ions could be chelated (Mulcahy et al. 2008). For instance, Priester et al. (2006) observed high amounts of eDNA associated with Cr(III), in *P. putida*. In our research, the highest content of eDNA (Cr(VI) and phenol treatments) was correlated to high Cr(VI) removal (around 50%), as well as to high Cr(VI) concentrations, in the exopolymer (around 1 mg L^{-1}). The remaining Cr(VI) removed from the liquid medium may be reduced to Cr(III) by chromate reductases and complexed by eDNA and EPS as well as internalized into cells (Fig. 3d). Results of the present study suggest that extracellular polysaccharides, proteins, and DNA could play an important role in the biofilm formation in *A. guillouiae* SFC 500-1A, as a response to simultaneous exposure to Cr(VI) and phenol.

Effect of Cr(VI), phenol, and both contaminants on biofilm formation

Biofilm formation was similar to control after Cr(VI) treatment, as shown in Fig. 4b. However, it increased significantly with phenol. These results were consistent with images obtained by SEM and AFM, which showed that the cells were aggregated forming a characteristic biofilm (Figs. 1e, g and 4e, f). There is not a general pattern of biofilm formation, because it is influenced by multiple factors, such as environmental stress and nutritional content of the medium (Dobinsky et al. 2003; Ryu et al. 2004; Kolter and Greenberg 2006; Busscher and Mei 2012). Biofilm formation is thought to begin when bacteria sense environmental conditions. These environmental signals vary among organisms. For instance, *Listeria monocytogenes* produced more biofilm in nutrient-rich media (Stepanovic et al. 2004), while *P. aeruginosa* and *P. fluorescens* formed biofilm under almost any condition that allows growth (O'Toole and Kolter 1998). Glucose promoted biofilm formation in *Staphylococcus aureus* (Rode et al. 2007), whereas phenol also increased biofilm formation in *A. guillouiae* SFC 500-1A, because this compound could be used as an extra source of carbon. Thus, biofilm formation would be a survival strategy of *A. guillouiae* SFC 500-1A under phenol treatment. However, exposure to Cr(VI) did not affect biofilm formation in this strain.

Despite different results, biofilm-mediated bioremediation represents a proficient and safer alternative than remediation with planktonic microorganisms, because cells in a biofilm have a better chance of adaptation and survival (especially during periods of stress) as they are protected within the matrix (Guibaud et al. 2006). In fact, due to the close, mutually beneficial physical and physiological interactions among microorganisms in biofilms, they are used in industrial plants to help in the immobilization and degradation of pollutants.

Cell hydrophobicity

The affinity of microbial cells for hydrophobic interfaces is an important property that directly affects the efficiency of various bioprocesses, such as bioremediation, waste treatment, and other technologies, using whole microbial cells (Hori et al. 2008). Although it is difficult to give a definition of hydrophobicity, some authors can explain the hydrophobic bond as a greater tendency for non-polar molecules to associate with other non-polar molecules, than to water (Doyle 2000).

The cell surface hydrophobicity of *A. guillouiae* SFC 500-1A growing in the presence of Cr(VI), phenol, or both contaminants, at different exposure times, was determined by measuring the percentage of cells adhered to the xylene phase. The percentage of hydrophobicity was 60%, regardless of the contaminant and exposure time. A removal of more than 50% of the cell suspension from the aqueous phase into the organic phase is indicative of the presence of a hydrophobic cell surface (Tahmourespour et al. 2008). The ability of bacterial cells to adhere to hydrocarbon is not restricted to hydrocarbon-degrading bacteria, suggesting that direct contact between cells and bulk hydrocarbon is due to general hydrophobic interactions (Rosenberg et al. 1980).

A change in cell hydrophobicity of *A. guillouiae* SFC 500-1A exposed to phenol might help to explain the increased biofilm production of bacteria in those conditions; however, no changes in cell hydrophobicity were observed after treatment. Probably, the contact with a moderately hydrophobic compound, such as phenol, favors that cells interact with each other (co-adhesion) and form biofilm, as was observed by AFM (Fig. 1e–h) and SEM images (Fig. 4e, f) and biofilm quantification (Fig. 4a). In this sense, Pompilio et al. (2008) reported that hydrophobic bacteria possess affinity to each other, leading to the self-assembly of bacteria with hydrophobic compounds. Several reports have shown that bacterial adhesion to surfaces is the first step in biofilm formation (Vuong and Otto 2002). Once adhered to a surface, bacteria aggregate to form microcolonies organized in a three-dimensional structure of biofilm. However, high levels of initial adherence do

not necessarily lead to thick biofilm formation (Cerca et al. 2005). It is clear that a large number of factors, besides cell surface hydrophobicity, are involved in biofilm formation, such as nutrient supply, hydrodynamic forces, surface charges, and presence of adhesion proteins, such as pili or flagella (Denkhaus et al. 2007). Moreover, Pompilio et al. (2008) showed that a similar biofilm formation ability may be found with strains displaying different hydrophobicity values. Thus, more knowledge is needed about bacterial components required for biofilm development as well as mechanisms that regulate their production and activity for a deep understanding of this microbial phenomenon.

Conclusion

The continuous changes of environmental conditions forces an adaptive modification in microorganisms which enhances their ability to survive. However, many of the mechanisms involved in this process are poorly known. The present study shows new evidences of some mechanisms displayed by *A. guillouiae* SFC 500-1A exposed to Cr(VI), phenol, and both contaminants simultaneously. Cr(VI) mainly induced intracellular changes, as well as an increase in protein and DNA content of the exopolymeric matrix. On the other hand, phenol produced changes at the membrane level, an increase in the extracellular production of protein and DNA, and also an increment in biofilm formation. In addition, changes at the membrane level and morphological and intracellular disturbances were observed after treatment with both contaminants. In such conditions, increases in EPS, protein, and DNA content of the exopolymer and biofilm formation were also detected. These changes reveal different adaptative responses used by bacterial cells to resist the effects of contaminants.

Thus, the combination of AFM with other techniques opens new perspectives on environmental microbiology, allowing to study bacterial dynamics and providing a more in-depth characterization of the effect of pollutants on bacteria, which will provide the basis for the development of better biotechnological strategies for cleaning up polluted environments.

Acknowledgements G.M.M., E.A., and P.S.G. are members of the research career from Consejo Nacional de Investigaciones Científicas y Técnicas (CONICET) (Argentina). M.F. has a fellowship from CONICET. We wish to thank PPI (SECyT-UNRC), CONICET, MinCyT Córdoba, and PICT (FONCyT) for the financial support.

References

Ackerley DF, Barak Y, Lynch SV et al (2006) Effect of chromate stress on *Escherichia coli* K-12. J Bacteriol 188:3371–3381

APHA-AWWA (1998) Standard methods for the examination of water and wastewater, 17th ed

ATSDR (2005) Agency for Toxic Substances and Disease Registry. Comprehensive Environmental Response, Compensation, And Liability Act (CERCLA) priority list of hazardous substances. http://www.atsdr.cdc.gov/cercla/05list.html

Batool R, Yrjälä K, Hasnain S (2014) Impact of environmental stress on biochemical parameters of bacteria reducing chromium. Braz J Microbiol 45:573–583

Bencosme SA, TsutSumi V (1970) Fast method for processing biologic material for electron microscopy. Lab Invest 23:447

Beringer JE (1974) R factor transfer in Rhizobiurn Zegurninosarum. J Gen Microbiol 84:188–198

Bhattacharya A, Gupta A (2013) Evaluation of Acinetobacter sp. B9 for Cr(VI) resistance and detoxification with potential application in bioremediation of heavy-metals-rich industrial wastewater. Environ Sci Pollut Res 20:6628–6637

Bhattacharya A, Gupta A, Kaur A (2014) Efficacy of Acinetobacter sp. B9 for simultaneous removal of phenol and hexavalent chromium from co-contaminated system. Appl Microbiol Biotechnol 98:9829–9841

Bradford MM (1976) A rapid and sensitive method for the quantitation of microgram quantities of protein utilizing the principle of protein-dye binding. Anal Biochem 254:248–254

Busscher HJ, Van Der Mei HC (2012) How do bacteria know they are on a surface and regulate their response to an adhering state? PLoS Pathog 8:1–4

Cerca N, Pier GB, Vilanova M et al (2005) Quantitative analysis of adhesion and biofilm formation on hydrophilic and hydrophobic surfaces of clinical isolates of *Staphylococcus epidermidis*. Res Microbiol 156:506–514

Das T, Sharma PK, Busscher HJ et al (2010) Role of extracellular DNA in initial bacterial adhesion and surface aggregation. Appl Environ Microbiol 76:3405–3408

Das T, Sharma PK, Krom BP et al (2011) Role of eDNA on the adhesion forces between Streptococcus mutans and substratum surfaces: influence of ionic strength and substratum hydrophobicity. Langmuir 27:10113–10118

Daulton TL, Little BJ, Lowe K, Jones-meehan J (2001) In situ environmental cell-transmission electron microscopy study of microbial reduction of chromium (VI) using electron energy loss spectroscopy. Microsc Microanal 7:470–485

Denkhaus E, Meisen S, Telgheder U, Wingender J (2007) Chemical and physical methods for characterisation of biofilms. Microchim Acta 158:1–27

Dhal B, Thatoi HN, Das NN, Pandey BD (2013) Chemical and microbial remediation of hexavalent chromium from contaminated soil and mining/metallurgical solid waste: a review. J Hazard Mater 250–251:272–291

Dische Z (1962) General color reactions. Methods Carbohydr Chem 1: 478–512

Dobinsky S, Kiel K, Rohde H et al (2003) Glucose-related dissociation between icaADBC transcription and biofilm expression by *Staphylococcus epidermidis*: evidence for an additional factor required for polysaccharide intercellular adhesin synthesis. J Bacteriol 185:2879–2886

Dogan NM, Doganli GA, Dogan G, Bozkaya O (2015) Characterization of extracellular polysaccharides (EPS) produced by thermal Bacillus and determination of environmental conditions affecting exopolysaccharide production. Int J Environ Res 9:1107–1116

Doyle RJ (2000) Contribution of the hydrophobic effect to microbial infection. Microbes Infect 2:391–400

Dubrovin EV, Popova AV, Kraevskiy SV et al (2012) Atomic force microscopy analysis of the Acinetobacter baumannii bacteriophage AP22 lytic cycle. 7:1–9

Dufrene YF (2008) Atomic force microscopy and chemical force microscopy of microbial cells. Nat Protocols 3:1132–1138

Dufrêne YF (2014) Atomic force microscopy in microbiology: new structural and functional insights into the microbial cell surface. MBio 5: 1–14

Fang HHP, Xu L, Chan K (2002) Effects of toxic metals and chemicals on biofilm and biocorrosion. Water Res 36:4709–4716

Farrell A, Quilty B (2002) Substrate-dependent autoaggregation of Pseudomonas putida CP1 during the degradation of monochlorophenols and phenol. J Ind Microbiol Biotechnol 28:316–324

Francisco R, Moreno A, Morais PV (2010) Different physiological responses to chromate and dichromate in the chromium resistant and reducing strain Ochrobactrum tritici 5bvl1. Biometals 23:713–725

Francius G, Lebeer S, Alsteens D et al (2008) Detection, localization, and conformational analysis of single polysaccharide molecules on live bacteria. Am Chem Soc 2:1921–1929

Guibaud G, Van Hullebusch E, Bordas F (2006) Lead and cadmium biosorption by extracellular polymeric substances (EPS) extracted from activated sludges: pH-sorption edge tests and mathematical equilibrium modelling. Chemosphere 64:1955–1962

Harish R, Samuel J, Mishra R et al (2012) Bio-reduction of Cr (VI) by exopolysaccharides (EPS) from indigenous bacterial species of Sukinda chromite mine, India. Biodegradation 23:487–496

He M, Li X, Guo L et al (2010) Characterization and genomic analysis of chromate resistant and reducing Bacillus cereus. BMC Microbiol 10:221

Hori K, Watanabe H, Ishii S et al (2008) Monolayer adsorption of a "bald" mutant of the highly adhesive and hydrophobic bacterium Acinetobacter sp. strain Tol 5 to a hydrocarbon surface. Appl Environ Microbiol 74:2511–2517

Hu Z, Jin J, Abruña HD et al (2007) Spatial distributions of copper in microbial biofilms by scanning electrochemical microscopy. Environ Sci Technol 41:936–941

Hung C, Warnken KW, Santschi PH (2005) A seasonal survey of carbohydrates and uronic acids in the Trinity River, Texas. Org Geochem 36:463–474

Kang Y, Park W (2010) Protection against diesel oil toxicity by sodium chloride-induced exopolysaccharides in Acinetobacter sp. strain DR1. JBIOSC 109:118–123

Kolter R, Greenberg EP (2006) Microbial sciences: the superficial life of microbes. Nature 441:300–302

Li J, Mclandsborough LA (1999) The effects of the surface charge and hydrophobicity of *Escherichia coli* on its adhesion to beef muscle. Int J Food Microbiol 53:185–193

Li B, Pan D, Zheng J et al (2008) Microscopic investigations of the Cr(VI) uptake mechanism of living Ochrobactrum anthropi. Langmuir 24:9630–9635

Liu HH, Yang YR, Shen XC et al (2008) Role of DNA in bacterial aggregation. Curr Microbiol 57:139

Longo G, Kasas S (2014) Effects of antibacterial agents and drugs monitored by atomic force microscopy. Wiley Interdiscip Rev Nanomed Nanobiotechnol 6:230–244

McLean J, Beveridge TJ (2001) Chromate reduction by a Pseudomonad isolated from a site contaminated with chromated copper arsenate. Appl Environ Microbiol 67:1076–1084

Molin S, Tolker-Nielsen T (2003) Gene transfer occurs with enhanced efficiency in biofilms and induces enhanced stabilisation of the biofilm structure. Curr Opin Biotechnol 14:255–261

Morris VJ, Kirby AR, Gunning AP (1999) Atomic force microscopy for biologists. Imperial College Press, London

Mueller K, González JE (2011) Complex regulation of symbiotic functions is coordinated by MucR and quorum sensing in Sinorhizobium meliloti. J Bacteriol 193:485–496

Mulcahy H, Charron-mazenod L, Lewenza S (2008) Extracellular DNA chelates cations and induces antibiotic resistance in Pseudomonas aeruginosa biofilms. PLoS Pathogens 4(11):1–12

O'Toole GA, Kolter R (1998) Initiation of biofilm formation in *Pseudomonas fluorescens* WCS365 proceeds via multiple, convergent signalling pathways: a genetic analysis. Mol Microbiol 28:449–461

Onbasli D, Aslim B (2009) Effects of some organic pollutants on the exopolysaccharides (EPSs) produced by some Pseudomonas spp. strains. J Hazard Mater 168:64–67

Ontañon OM, González PS, Agostini E (2015) Biochemical and molecular mechanisms involved in simultaneous phenol and Cr(VI) removal by Acinetobacter guillouiae SFC 500-1A. Environ Sci Pollut Res 17:13014–13023

Pal A, Paul AK (2008) Microbial extracellular polymeric substances: central elements in heavy metal bioremediation. Indian J Microbiol 48:49–64

Pompilio A, Piccolomini R, Picciani C et al (2008) Factors associated with adherence to and biofilm formation on polystyrene by Stenotrophomonas maltophilia: the role of cell surface hydrophobicity and motility. FEMS Microbiol Lett 287:41–47

Priester JH, Olson SG, Webb SM et al (2006) Enhanced exopolymer production and chromium stabilization in Pseudomonas putida unsaturated biofilms. Appl Environ Microbiol 72:1988–1996

Prieto Contreras LF, Alvelar Gonzáles FJ, Loera Muro VM et al (2015) Bioflocks structure from enriched lab-scale stabilization ponds used to remove high chromium concentrations. Int J Curr Microbiol App Sci 4:625–634

Quintelas C, da Silva VB, Silva B et al (2011) Optimization of production of extracellular polymeric substances by Arthrobacter viscosus and their interaction with a 13X zeolite for the biosorption of Cr(VI). Environ Technol 32:1541–1549

Rode MT, Langsrud S, Holck A, Møretrø T (2007) Different patterns of biofilm formation in *Staphylococcus aureus* under food-related stress conditions. Int J Food 116:372–383

Rosenberg M, Gutnick D, Rosenberg E (1980) Adherence of bacteria to hydrocarbons: a simple method for measuring cell-surface hydrophobicity. FEMS Microbiol Lett 9:29–33

Ryu JH, Kim H, Beuchat LR (2004) Attachment and biofilm formation by *Escherichia coli* O157:H7 on stainless steel as influenced by exopolysaccharide production, nutrient availability, and temperature. J Food Prot 67:2123–2131

Salehizadeh H, Shojaosadati SA (2003) Removal of metal ions from aqueous solution by polysaccharide produced from Bacillus firmus. Water Res 37:4231–4235

Samuel J, Paul ML, Pulimi M et al (2012) Hexavalent chromium bioremoval through adaptation and consortia development from Sukinda chromite mine isolates. Ind Eng Chem Res 51:3740–3749

Santamaría M, Díaz-Marrero AR, Hernández J et al (2003) Effect of thorium on the growth and capsule morphology of Bradyrhizobium. Environ Microbiol 5:916–924

Sharma SK, Petrusevski B, Amy G (2008) Chromium removal from water: a review. J Water Supply Res Technol AQUA 57:541–553

Sheng GP, Yu HQ, Yue ZB (2005) Production of extracellular polymeric substances from Rhodopseudomonas acidophila in the presence of toxic substances. Appl Microbiol Biotechnol 69(2):216–22

Sidek MSBM (2010) The removal of chromium (VI) and phenol from industrial waste waters mediated by Acinetobacter haemolyticus. Universiti Teknologi Malaysia

Srivastava S, Thakur IS (2007) Evaluation of biosorption potency of Acinetobacter sp. for removal of hexavalent chromium from tannery effluent. Biodegradation 18:637–646

Steinberger RE, Holden PA (2005) Extracellular DNA in single- and multiple-species unsaturated biofilms. Appl Environ Microbiol 71: 5404–5410

Stepanovic S, Cirkovic I, Ranin L, Svabic M (2004) Biofilm formation by Salmonella spp. and *Listeria monocytogenes* on plastic surface. Lett Appl Microbiol 38:428–432

Strelkova EA, Pozdnyakova NV, Zhurina MV et al (2013) Role of the extracellular polymer matrix in resistance of bacterial biofilms to extreme environmental factors. Microbiology 82:119–125

Tahmourespour A, Kermanshahi RK, Salehi R, Nabinejad A (2008) The relationship between cell surface hydrophobicity and antibiotic resistance of streptococcal strains isolated from dental plaque and caries. Irian J Basic Med Sci 10:251–255

Vuong C, Otto M (2002) *Staphylococcus epidermidis* infections. Microbes Infect 4:481–489

Wagner M, Nicell JA (2002) Detoxification of phenolic solutions with horseradish peroxidase and hydrogen peroxide. Water Res 36:4041–4052

Zakaria ZA, Mat Jais AM, Mastura M et al (2007) In vitro antistaphylococcal activity of the extracts of several neglected plants in Malaysia. Int J Pharmacol 3:428–431